Cadmium isotopic constraints on metal sources in the Huize Zn–Pb deposit, SW China

Chuanwei Zhu, Hanjie Wen, Yuxu Zhang, Zhilong Huang, Christophe Cloquet, Béatrice Luais, Tao Yang

Geoscience Frontiers 12 (2021) 101241

HOSTED BY

Contents lists available at ScienceDirect

Geoscience Frontiers

journal homepage: www.elsevier.com/locate/gsf

Research Paper

Cadmium isotopic constraints on metal sources in the Huize Zn–Pb deposit, SW China

Chuanwei Zhu [a], Hanjie Wen [a,b,*], Yuxu Zhang [a], Zhilong Huang [a], Christophe Cloquet [c], Béatrice Luais [c], Tao Yang [d]

[a] State Key Laboratory of Ore Deposit Geochemistry, Institute of Geochemistry, Chinese Academy of Sciences, Guiyang 550081, China
[b] University of Chinese Academy of Sciences, Beijing 100049, China
[c] Centre de Recherches Petrographiques et Geochimiques, CNRS/UMR 7358, 15, Rue Notre-Dame-Pauvres, B. P. 20, 54501 Vandoeuvre-les-Nancy Cedex, France
[d] State Key Laboratory for Mineral Deposits Research, Department of Earth Sciences, Nanjing University, Nanjing 210093, China

ARTICLE INFO

Article history:
Received 23 February 2021
Revised 15 May 2021
Accepted 26 May 2021
Available online 28 May 2021
Handling Editor: C.J. Spencer

Keywords:
Cd isotopes
Sulfide
Hydrothermal system
Huize Zn–Pb deposit

ABSTRACT

The Sichuan–Yunnan–Guizhou (SYG) Zn–Pb metallogenic zone in SW China contains >400 carbonate-hosted hydrothermal Zn–Pb deposits. Some of these, such as the Huize, Tianbaoshan, and Daliangzi deposits, are super-large deposits with significant reserves of Cd, Ge, and Ag. However, the sources of these metals remain controversial. This study investigated the Cd isotopic geochemistry of the Huize deposit, the largest Zn–Pb deposit in the SYG area. Sphalerites formed at three stages in the deposit have different colors: black or dark brown (Stage I), red (Stage II), and light-yellow (Stage III). The $\delta^{114/110}$Cd values of the sphalerites are in the order Stage III < Stage I < Stage II. Kinetic isotopic fractionation is likely the key factor causing the lower $\delta^{114/110}$Cd values in the early formed Stage I sphalerites than in later-formed Stage II sphalerites, with cooling of ore-forming fluids being responsible for the still lower values of the Stage III sphalerites. In galena, the $\delta^{114/110}$Cd values are inversely correlated with Cd contents and tend to be higher in high-Zn galena. We speculate that Cd isotopic fractionation was significant during the precipitation of sphalerite and galena, with light Cd isotopes being enriched in galena rather than sphalerite. Comparison of the Cd isotopic signatures and Zn/Cd ratios of different endmembers suggests that the $\delta^{114/110}$Cd values and Zn/Cd ratios of sphalerite from the Huize deposit, as well as other large-scale deposits from the SYG area, are lie in those range of Emeishan basalts and sedimentary rocks and the mean $\delta^{114/110}$Cd values of these deposits show good negative correlation with 1/Cd, suggesting that the ore-forming materials of these deposits were derived from the mixing of Emeishan basalts and sedimentary rocks. This study demonstrates that Cd isotopes can be useful proxies in elucidating ore genesis in large Zn–Pb deposits.

1. Introduction

Cadmium (Cd) has eight natural stable isotopes (^{106}Cd, ^{108}Cd, ^{110}Cd, ^{111}Cd, ^{112}Cd, ^{113}Cd, ^{114}Cd, and ^{116}Cd) and its isotopic geochemistry provides insights into its sources and geochemical processes in terrestrial and extraterrestrial systems (e.g., Wombacher et al., 2003, 2008; Ripperger et al., 2007; Ripperger and Rehkämper, 2007; Schmitt et al., 2009a; Rehkämper et al., 2012; Zhu et al., 2015). Mass-dependent fractionation of Cd isotopes has been observed in geochemical processes such as evaporation and condensation (Wombacher et al., 2004), precipitation (Horner et al., 2011; Zhu et al., 2013, 2017), adsorption (Wasylenki et al., 2014), and biological processes (Lacan et al., 2006; Wei et al., 2016; Wiggenhauser et al., 2016; Li et al., 2019). Large variations in $\delta^{114/110}$Cd values (>3‰) have been reported in rocks (Wombacher et al., 2003; Schmitt et al., 2009a; Georgiev et al., 2015; Hohl et al., 2017, 2019; Zhang et al., 2018), ore deposits (Zhu et al., 2013, 2016; Wen et al., 2016; Li et al., 2019), soils (Cloquet et al., 2006; Chrastný et al., 2015; Wen et al., 2015), sediments (Gao et al., 2008; Zhang et al., 2016), seawater (Ripperger et al., 2007; Abouchami et al., 2011, 2014; Yang et al., 2012), and biological samples (Wei et al., 2016; Wiggenhauser et al., 2016). With the isotopic signatures of different source endmembers being well defined, it has been possible to trace and quantify sources of

* Corresponding author at: State Key Laboratory of Ore Deposit Geochemistry, Institute of Geochemistry, Chinese Academy of Sciences, Guiyang 550081, China.
E-mail address: wenhanjie@vip.gyig.ac.cn (H. Wen).

https://doi.org/10.1016/j.gsf.2021.101241

Cd in various environments, using Cd-isotope-based mixing models (Cloquet et al., 2006; Lambelet et al., 2013; Abouchami et al., 2014; Wen et al., 2015). Wen et al. (2016) investigated Cd isotopic fractionation in different types of hydrothermal system, and found that high-temperature systems have lower $\Delta^{114/110}$Cd value (~0.4‰) than Mississippi Valley Type (MVT) deposits (~1.5‰), and that the mean $\delta^{114/110}$Cd value of magma-related deposits (0.08‰ ± 0.21‰; 2SD) is similar to that of basalts (0.00 ± 0.08‰; Liu et al., 2019; Tan et al., 2020), suggesting that sphalerite inherited the Cd isotopic signatures of source beds. In MVT deposits, biological processes and mineral precipitation are considered important factors causing strong Cd isotopic fractionation in such systems (Zhu et al., 2017; Li et al., 2019). Although Cd isotopic fractionation mechanisms have been widely studied in different hydrothermal systems, the Cd isotopic signatures of potential source beds are still unclear in medium–low-temperature hydrothermal systems, restricting the application of Cd isotopes in tracing metal sources in such systems. Further studies are therefore needed to extend the application of Cd isotopes in large hydrothermal systems.

We investigated the isotopic geochemistry of Cd in the Huize deposit in the Sichuan–Yunnan–Guizhou (SYG) metallogenic area of SW China. As a world-class Zn–Pb metallogenic zone, the SYG area is defined as a low-temperature metallogenic domain (generally below 200–250 °C) containing more than 400 carbonate-hosted hydrothermal Zn–Pb deposits with total Zn and Pb ore reserves of >150 million tons at average grades of 10 wt.% Zn and 5 wt.% Pb (Zaw et al., 2007; Ye et al., 2011; Zhang et al., 2015). As the most representative and largest Zn–Pb deposit in the SYG area, the Huize deposit has been intensively studied, but its origin remains controversial. Geologically, the deposit is hosted by carbonate rocks and was therefore suggested to be an MVT ore deposit (Zhou et al., 2001; Han et al., 2007; Zhang et al., 2015). However, recent studies of geological settings, fluid inclusions, trace elements, and S and Pb isotopes have suggested that the deposit may differ from typical MVT deposits (Huang et al., 2004; Zhang et al., 2005; Han et al., 2007, 2017; Zhou et al., 2013a; Zhu et al., 2016). The Huize deposit is spatially and intimately associated with the Emeishan large igneous province (259–251 Ma; Zhou et al., 2002; Zhong et al., 2014), and numerous studies have argued that it may be a magma-related deposit and that Emeishan flood basalts may be an important source of the ore-forming fluids and metals (Li et al., 2007; Xu et al., 2014; Zhu et al., 2007; Huang et al., 2004).

We investigated the Zn and Cd contents and Cd isotopic compositions of sulfides, sedimentary rocks, and igneous rocks collected from the Huize ore deposit with the aim of elucidating the ore genesis of the Huize deposit.

2. Geology of the Huize deposit

The SYG metallogenic area lies at the junction of the Yangtze, Cathaysia, and Indochina blocks (Fig. 1a). Strata in the area include basement and sedimentary cover. From lower to uppermost, the basement comprises the Paleoproterozoic Kangding (Pt_1^1k; migmatite and gneiss) and Dahongshan (Pt_1^2d; meta-clastic rock and spilite-keratophyre sequence) groups, and the Meso-Neoproterozoic Kunyang Group ($Pt_{2\text{-}3}k$; clastic rock with minor carbonate; Zhou et al., 2001; Huang et al., 2004). The sedimentary cover includes (in ascending stratigraphic order) Ediacaran to Quaternary strata comprising predominantly limestone and dolomite. Emeishan flood basalts (late Permian) cover an area of >250,000 km^2 with a total thickness ranging from several hundred meters to 5 km and are widely distributed in the SYG area (Zhou et al., 2001; Fig. 1). These flood basalts are commonly overlain by Triassic sedimentary rocks and underlain by the middle Permian Qixia–Maokou Formation. Geographic and geological investigations have shown that the SYG Zn–Pb deposits are carbonate-hosted ore deposits, which are commonly located near deep-seated regional faults and spatially associated with fault intersections and Emeishan basalts (Huang et al., 2004; Fig. 1b).

The Huize deposit lies at the intersection of NE- and NS-trending tectonic belts between (from north to south) the Zhaotong–Qujing concealed fault zone and the Xiaojiang fault zone (Fig. 1b). Orebodies occur within the Kuangshanchang fault zone in the southwestern segment of the Dongchuan–Zhenxiong region related to the major Xiaojiang and Zhaotong–Qujing faults (Fig. 1b). Outcrops in the Huize deposit are hosted by Ediacaran to Permian strata comprising mainly carbonaceous rocks (Fig. 2). The Huize deposit includes two principal mines, namely the Kuangshanchang and Qilinchang mines, with the No. 1 orebody of the former and the Nos. 3, 6, 8, and 10 orebodies of the latter containing >90% of the total metal reserves of the Huize deposit (Huang et al., 2004; Yin et al., 2009). Orebodies of both the Kuangshanchang and Qilinchang mines are all in the Baizuo Formation (lower Carboniferous, C_1b), which comprises predominantly light–yellow and red coarse dolomite interbedded with gray limestone and dolomitic limestone (Fig. 2). The orebodies are lenticular, chambered, and veined. The Huize deposit contains >6 million tons of total metal reserves with a combined Zn and Pb grade of ~30 wt.% (Han et al., 2015). It is also enriched in Ag, Ge, and Cd at up to 200 μg g^{-1}, 81 μg g^{-1}, and 488 μg g^{-1} in Zn–Pb ores, respectively (Han et al., 2007).

The economic minerals of the Huize deposit include mainly sphalerite and galena (Supplementary Data, Fig. S1A), similar to other Zn–Pb deposits in the SYG area. Predominant ore textures are subhedral–euhedral granular, metasomatic–resorption, and fracture-infill textures (Huang et al., 2004). Sphalerite is euhedral to anhedral with grain sizes of 1–30 mm, and commonly coexists with galena, pyrite, calcite, and dolomite (Supplementary Data, Fig. S1B–F). Different shades of sphalerite colors can be distinguished in hand specimens. Detailed microscopic observations indicate that color zonation patterns occur throughout the entire sphalerite crystal, with the color changing continuously from dark at the core to pale at the edge (Supplementary Data, Fig. S1; Li and Zhu, 2020). Dark sphalerite is commonly rounded and/or crossed by pale sphalerite (Supplementary Data, Fig. S1A) with its formation thus being divided into different stages based on color: Stage I, the initial stage with black or dark-brown color; Stage II, the middle stage with red or pale-brown color; and Stage III with light-yellow color. Galena is euhedral to anhedral with grain sizes of 10 μm to 20 mm, is commonly intergrown with sphalerite, and generally precipitated later than sphalerite (Supplementary Data, Fig. S1B–E). Gangue minerals include mainly pyrite, calcite, and dolomite. Pyrites are commonly euhedral and were deposited earlier than sphalerite and galena. Calcites and dolomites were generally precipitated later than the sulfides, but some were formed earlier than galena (Huang et al., 2004). Detailed signatures of these minerals are shown in Supplementary Data (Fig. S1).

Five and three representative hand specimens, respectively, were collected from the No. 8 and No. 10 orebodies of the Huize deposit. Different-colored sphalerites were collected from these specimens to provide time constraints on the variation of Cd isotopic composition during sphalerite precipitation. Five galena samples were selected for comparison of Cd isotopic fractionation between sulfides. Twenty sedimentary rocks and two Emeishan basalts were collected from a typical stratigraphic section located ~7 km from the Huize deposit. Sedimentary rocks include siltstone, sandstone, limestone, shale, and dolomite that were deposited during the Devonian–Permian.

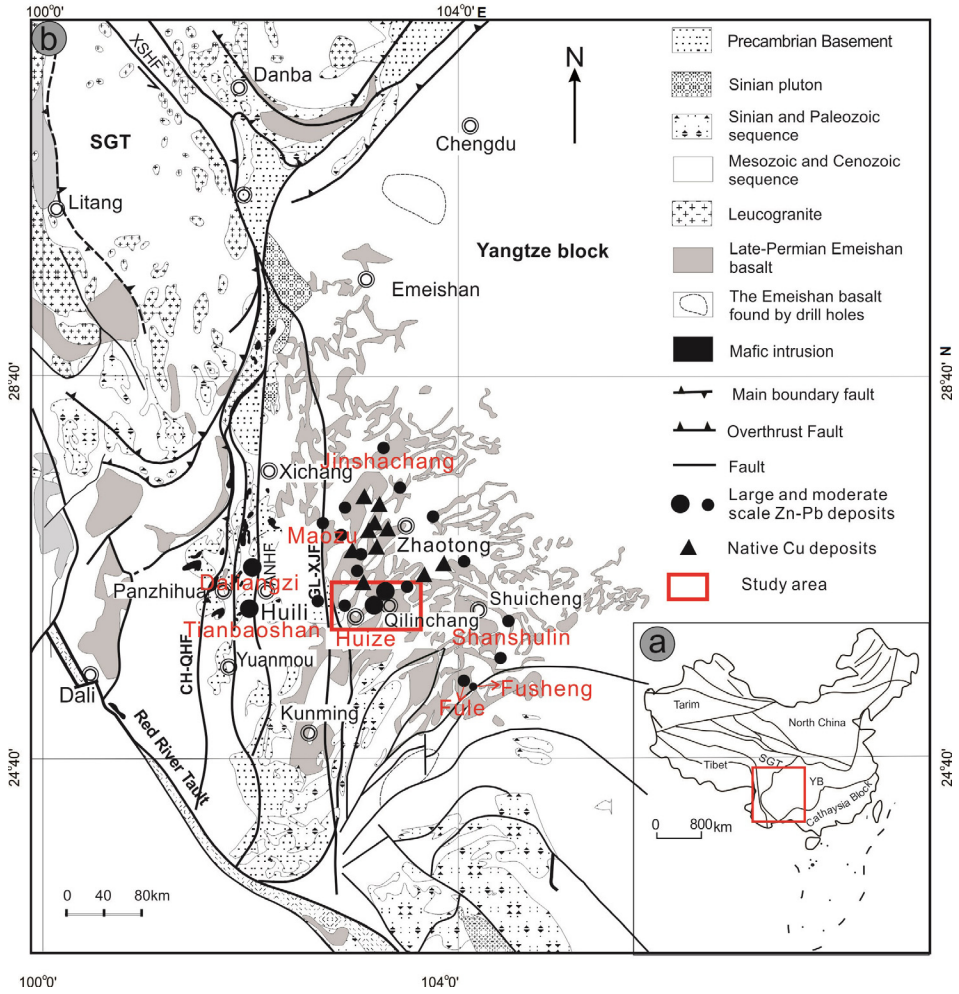

Fig. 1. (a) Tectonic sketch and (b) regional geological map of the SYG Zn–Pb metallogenic province, SW China (modified from Zhu et al., 2017).

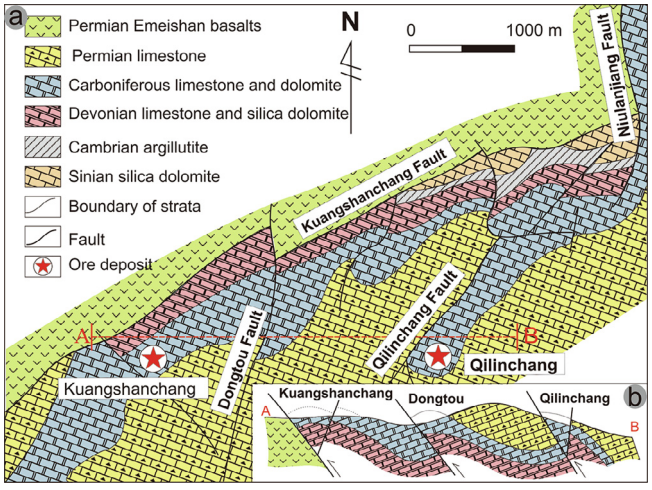

Fig. 2. Geological map (a) and typical cross-section (b) of the Huize Zn–Pb deposit (modified from Huang et al., 2004).

3. Methods

3.1. Sample preparation

Sulfides were crushed into 40–60 mesh, and 4 galena and 18 sphalerite samples of different colors were handpicked under a binocular microscope. The selected mineral separates were then crushed to ~200 mesh. Sedimentary rocks and basalts were washed with distilled water, air-dried, and crushed to ~200 mesh.

3.2. Sample digestion and chemical purification

Cadmium isotopic compositions of sulfides and rock samples were determined in 2013 and 2017, respectively, with separate methods being employed for Cd purification due to their different Cd contents (Table 1). For sulfides, ~100 mg of sphalerite (~200 mg for galena) was weighed into a 7 mL Teflon digestion vial (Savilex; USA). The samples were then reacted with 3 mL concentrated HNO_3 at 110 °C for 24 h. After evaporation to dryness, each sample was digested in 1 mL concentrated HF and evaporated to dryness at 110 °C. Sulfide samples were purified on columns containing 3 mL pre-cleaned 100–200 mesh AG MP-1 M (Bio-Rad, USA) anion-exchange resin (Table 1) using the method of Zhu et al. (2013), which yielded Cd recoveries of >98%.

For rock samples, sub-samples containing ~150 ng Cd were placed in 50 mL Teflon digestion vials, digested with 10 mL aqua regia, and heated to dryness at 180 °C over ~24 h, with the residue then being dissolved in 10 mL 1% HNO_3. A ^{111}Cd–^{110}Cd double-spike solution ($^{111}Cd/^{110}Cd \approx 2$) was added to each sample to achieve a Cd spike–sample ratio of ~2. The samples were then mechanically shaken for 24 h to reach Cd isotopic equilibrium. Each sample was then transferred to a centrifuge tube and centrifuged for 20 min (4000 rpm). The residue was reacted with

Table 1
Sample digestion and column chemistry protocol.

Sulfide sample digestion	Sedimentary rocks digestion
2 mL 15 M HNO_3, evaporation	10 mL aqua regia, evaporation
1 mL HF, evaporation	Dissolved in 10 mL 1% HNO_3 + double spike solution, centrifugation and evaporation
Dissolved in 2mL 2 M HCl	Dissolved in 3mL 2 M HCl
Resin	Resin
3 mL AG MP-1 M (100–200 mesh)	3 mL AG MP-1 M (100–200 mesh)
Preconditioning resin	Preconditioning resin
10 mL 2 M HCl	10 mL 2 M HCl
Elution	Elution
Load sample in 2 mL, 2 M HCl	Load sample in 3 mL, 2 M HCl
10 mL 2 M HCl, elute matrix elements	10 mL 2 M HCl, elute matrix elements
30 mL 0.3 HCl, elute Pb	30 mL 0.3 HCl, elute Pb
20 mL 0.06 HCl, elute Sn	20 mL 0.06 HCl, elute Sn
5 mL 0.012 HCl, elute Zn and Sn	5 mL 0.012 HCl, elute Zn and Sn
20 mL 0.0012 HCl, collect Cd	20 mL 0.0012 HCl, collect Cd
All collected solution evaporated and then dissolved in 2 mL 1% HNO_3 for analysis	All collected solution evaporated and then dissolved in 2 mL 2 M HCl for the secondary separation After twice separation, all collected solution evaporated and then dissolved in 2 mL 1% HNO_3 for analysis

5–10 mL concentrated HF at 180 °C over ~24 h. After evaporation, the supernatant and the digested residue of each sample were mixed for Cd purification. The chemical separation and purification methodologies for Cd of sedimentary rocks and sulfides were similar. Due to the low Cd contents of the sedimentary and igneous rocks, each sample was purified twice to achieve complete Cd separation from the matrix (Table 1); Cd recovery was >85%.

The double-spike solution was prepared from individual ^{110}Cd (CdO; 96.0% ± 0.3% purity) and ^{111}Cd (CdO; 96.18% ± 0.02% purity) spikes (Oak Ridge National Laboratory, USA). The Cd isotopic ratios of the double-spike solution were determined by long-term multi-collector inductively couple plasma mass spectrometry (MC-ICP-MS) analyses over more than six months at the Institute of Geochemistry, Chinese Academy of Sciences, Guiyang, China. Instrumental mass bias was corrected by external normalization using an Ag isotopic standard (US National Institute of Standards and Technology, (NIST) standard reference material (SRM) 978a; $^{107}Ag/^{109}Ag$ = 1.07638 ± 0.00022) using the exponential law. The Cd isotopic ratios of the double-spike solution are reported in Table 2.

All acids used in the study were prepared by sub-boiling distillation. Millipore 18.2 MΩ cm water was used throughout. The Cd standards, including NIST-3108 and Nancy Spex (CRPG, France), were used to monitor Cd isotopic fractionation during chemical separation and MS analyses.

3.3. Elemental and isotopic analyses

The Cd and Zn contents of the digested sulfides and trace-element contents of sedimentary rocks were determined at the Institute of Geochemistry, Chinese Academy of Science, by ICP–optical emission spectrometry (ICP-OES; Varian Vista MPX, USA) and ICP-MS (ElAN DRC-e, Perkin Elmer, USA), respectively. Uncertainties of the two methods were <10%, based on in-house standards.

Cadmium isotopic compositions of sulfides were determined by MC-ICP-MS (Neptune Plus, Thermo Fisher, USA) at the State Key Laboratory of Crust–Mantle Evolution and Mineralization, Nanjing University, Nanjing, China. The standard–sample bracketing method was used as suggested previously (Zhu et al., 2017). Cadmium isotopic compositions of sedimentary and igneous rocks were determined by MC-ICP-MS (Neptune Plus) at the State Key Laboratory of Ore Deposit Geochemistry, Institute of Geochemistry, Chinese Academy of Sciences. Detailed information on instrumentation and measurement protocols for the double-spike technique were reported by Zhang et al. (2018). A MATLAB-based script with an iterative double-spike correction algorithm was applied offline to compute Cd isotopic compositions of the double-spiked samples. Duplicate measurements of the international basalt standard BCR-2 (US Geological Survey) were performed for testing accuracy and reproducibility.

Cadmium isotopic ratios are expressed in standard delta notation in per mil units relative to the NIST SRM 3108 Cd solution:

$$\delta^{x/110}Cd(‰) = [(^{x}Cd/^{110}Cd)_{sample}/(^{x}Cd/^{110}Cd)_{NIST\text{-}3108} - 1] \times 1000$$

where ^{x}Cd represents the ^{111}Cd, ^{112}Cd, and ^{114}Cd isotopes. Nancy Spex and Münster Cd were used as in-house standards during sample analyses, with NIST 3108Cd as the bracketing standard. Average values of $\delta^{114/110}Cd$ of Münster Cd and Nancy Spex Cd were 4.49‰ ± 0.09‰ (2SD; n = 4) and −0.12‰ ± 0.03‰ (2SD; n = 4), consistent with the previously reported values of 4.50‰ ± 0.05‰ and −0.09‰ ± 0.04‰, respectively (Abouchami et al., 2013). The measured $\delta^{114/110}Cd$ value of BCR-2 was −0.07‰ ± 0.08‰, consistent with published values within error (0.02‰ ± 0.04‰, Liu et al., 2019; and −0.01‰ ± 0.05‰, Tan et al., 2020).

4. Results

The Zn and Cd contents and Cd isotopic compositions of sulfides are listed in Supplementary Data (Table S1). Sphalerites have variable Zn and Cd contents of 46.4%–60.4% and 909–2440 μg g^{-1}, respectively. Zn and Cd contents of black and red sphalerites are negatively correlated (Fig. 5a), suggesting that Cd entered the sphalerite lattice through direct substitution of Zn^{2+} by Cd^{2+}, as suggested previously (Cook et al., 2009). Interestingly, dark sphalerite in the Huize deposit is commonly wrapped in pale sphalerite (Supplementary Data, Fig. S1A), and the color shades may be used to constraint the formation sequence (Huang et al., 2004; Han et al., 2007; Li and Zhu, 2020). As shown in Fig. 5b, all black sphalerites have higher Cd contents than red sphalerites, suggesting that earlier formed sphalerite (dark) has higher Cd content than the later formed type (red). However, light-yellow sphalerites do not obey this rule.

Galenas have low Zn and Cd contents of 0.02%–0.70% and 6–27 μg g^{-1}, respectively. The $\delta^{114/110}Cd$ values of sphalerites and galenas range from −0.17‰ to 0.36‰ and from −0.36‰ to 0.18‰, respectively. Sulfides were collected from separate mining levels of the No. 8 and No. 10 orebodies, but no clear Zn/Cd ratio or

Table 2
The average value of Cd isotopic ratios in double spike solution and NIST SRM 3108 Cd.

Solution	n	$^{111}Cd/^{110}Cd$	$^{112}Cd/^{110}Cd$	$^{114}Cd/^{110}Cd$
NIST 3108Cd	72	1.02596 ± 0.00018	1.93308 ± 0.00029	2.30434 ± 0.00046
^{110}Cd-^{111}Cd double spike	72	1.85110 ± 0.00031	0.0498434 ± 0.0000020	0.0165181 ± 0.0000022

n: number of measurements. Data resource: Zhang et al. (2018).

Cd isotopic differences were observed between levels (Supplementary Data, Table S1 and Fig. 3).

The Cd and Zn contents and $\delta^{114/110}$Cd values of sedimentary rocks and basalts are given in Supplementary Data (Table S2). The Emeishan basalts have higher Zn contents (99–136 μg g^{-1}) than those of sedimentary rocks (5–66 μg g^{-1}), but lower Cd contents (0.11–0.18 μg g^{-1}) than those of most sedimentary rocks (0.13–0.76 μg g^{-1}; Supplementary Data, Table S2; Fig. 4). Narrow ranges of $\delta^{114/110}$Cd values were observed in the Emeishan basalts (−0.13‰ to −0.22‰). In contrast, sedimentary rocks exhibit wide variations in $\delta^{114/110}$Cd values (−0.25‰ to 0.82‰). The $\delta^{114/110}$Cd values increase slightly from Devonian to Permian strata (Fig. 4; Supplementary Data, Table S2), largely overlapping with data previously published for sphalerite from Zn–Pb deposits in the SYG area, such as the Huize (−0.17‰ to 0.36‰, this study), Fule (0.17‰–0.81‰; Zhu et al., 2017), Tianbaoshan (0.12‰–0.68‰; Zhu et al., 2016), Daliangzi (0.02‰–0.56‰; Xu et al., 2019), Maozu (0.07‰–0.22‰; Xu et al., 2019), Jinshachang (0.20‰–0.33‰; Xu et al., 2019) and Fusheng (0.19‰–0.65‰; Xu et al., 2019) deposits.

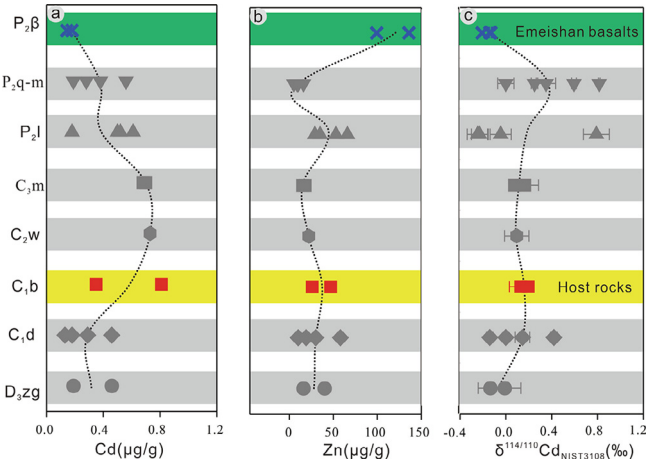

Fig. 4. Cd (a) and Zn (b) contents, and Cd isotopic compositions (c) of sedimentary rocks and Emeishan basalts sampled in the Huize ore district. Dashed lines indicate mean values of the Devonian (D_3zg) to Permian ($P_2\beta$) period (Y axis).

5. Discussion

5.1. Geochemistry of sphalerite

Previous Cd isotopic studies have indicated the preferential precipitation of isotopically lighter Cd in sulfides than in solutions, with the $\delta^{114/110}$Cd values of newly formed sulfides tending to increase with time (Yang et al., 2014; Zhu et al., 2017). Most dark sphalerites (Stage I) have lower $\delta^{114/110}$Cd values than the red type (Stage II; e.g., sample HZ-53; Supplementary Data, Table S1), consistent with previous studies (Zhu et al., 2017). However, the light-yellow sphalerites (Stage III) have lower $\delta^{114/110}$Cd values than both the dark and red types (e.g., samples HZ-25, 32, 34, 36; Supplementary Data, Table S1). In a study of the Tianbaoshan Pb–Zn deposit, dark sphalerites also exhibited higher $\delta^{114/110}$Cd values than the pale type (Zhu et al., 2016), which was explained as being due to the heterogeneous composition of ore-forming fluids. However, the lack of Pb isotopic variation in the ores suggests that ore-forming fluids were homogeneous in the Huize deposit (Zhou et al., 2001; Huang et al., 2004; Han et al., 2007). Rare-earth element (REE) and C–O isotopic signatures also suggest that ore-forming fluids were homogenized before mineralization (Huang et al., 2003, 2010). Furthermore, recent Zn isotopic data indicate minor Zn isotopic variation in sphalerite between different mining levels and orebodies of the Huize deposit, with $\delta^{66}Zn_{JMC}$ values ranging from 0.17‰ to 0.32‰ (Wu, 2013). Heterogeneity in fluid elemental and isotopic compositions is thus unlikely to explain the Cd isotopic variation between the pale-yellow and black or red sphalerites of the Huize deposit.

A few studies have documented factors that may be considered in accounting for the Cd isotopic signatures of sphalerite, such as Cd species in ore-forming fluids and fluid temperature (Schmitt et al., 2009b; Yang et al., 2014), with the latter being proven a crucial factor causing strong isotopic fractionation (Yang et al., 2014). Dark sphalerite is usually formed at higher temperatures than the pale type (Graeser, 1969). Infrared microthermometry of fluid inclusions in Huize sphalerite indicates homogenization temperatures of sphalerite-hosted fluid inclusions of 100–364 °C (Supplementary Data, Table S3), with that of inclusions in dark sphalerite being higher than in the pale type (Han et al., 2016). Yang et al. (2014) calculated the equilibrium isotopic fractionation between different Cd species at various temperatures in hydrothermal fluids and suggested that temperature variations may produce strong fractionation of up to 0.35‰ for $CdHS^+$ at 100–400 °C, slightly higher than the observed fractionation between distinct-colored sphalerites in hand specimens (up to 0.31‰; sample HZ-34). We suggest that kinetic isotopic fractionation resulted

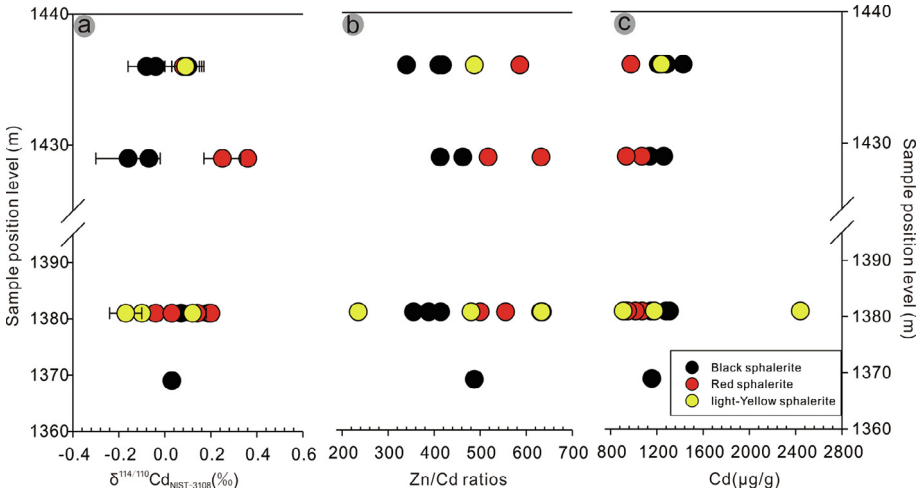

Fig. 3. Cd isotopic compositions (a), Zn/Cd ratios (b), and Cd contents (c) of different-colored sphalerite from the four mining levels of the Huize deposit.

in the early-formed black sphalerites with lower $\delta^{114/110}$Cd values than the later-formed red type, with temperature variations being a key factor causing the pale-yellow type to have lower $\delta^{114/110}$Cd values than both the dark and red types. This may also be supported by the higher homogenization temperature of inclusions in dark sphalerite than in the pale type (Han et al., 2016), resulting in the chemical signatures of light-yellow sphalerites being different to those of black and red sphalerites (Fig. 5a and b).

5.2. Geochemistry of galena

Previous studies have suggested that Cd could be incorporated into galena as chemically adsorbed compounds (Tauson et al., 2005) following isovalent substitution ($(Cd,Hg)^{2+} \leftrightarrow Pb^{2+}$; George et al., 2015). Linear positive correlation between Cd and Zn concentrations in galena have been observed in the Fule deposit, China (Zhu et al., 2017) and in the Alcudia Valley mineral field, Spain (Palero-Fernández and Martín-Izard 2005), suggesting that Cd occurs predominantly as sphalerite micro-inclusions in galena. In the Huize deposit, the galena Cd content is also strongly correlated with the Zn content (R^2 = 0.91; Fig. 5c), although we cannot exclude the possibility that Cd substitutes into the crystal lattice of galena, for the following two reasons. (1) Most galenas have lower Zn/Cd ratios (33–342) than those of sphalerites (235–635); if the Cd was derived only from sphalerite micro-inclusions, the galenas should have similar Zn/Cd ratios to those of sphalerites, as observed previously (Zhu et al., 2017). (2) The $\delta^{114/110}$Cd values are negatively correlated with the reciprocal of Cd content (1/Cd) in galena (R^2 = 0.62; Fig. 5d), implying a mixing of Cd in sphalerite micro-inclusions and isomorphism of Cd in galena. Meanwhile, Cd isotopes are significantly fractionated during the formation of sphalerite and galena (sample HZ-34) at hand-specimen scale with $\Delta^{114/110}Cd_{galena\text{-}sphalerite}$ values of up to ~0.50‰, suggesting that lighter Cd isotopes are preferentially enriched in galena over sphalerite. Crystal structures were considered as an important factor that controls isotope signatures between minerals (O'Neil, 1977). However, due to limited studies, it is still unclear the reason that light Cd isotopes preferred to enrich in galena rather than sphalerite, thus, we could not give further explanations on this conclusion.

5.3. Metal sources in Huize and other deposits in the SYG area

As Group IIB transition metals, Cd and Zn have similar electronic structures and ionization potentials, and therefore similar geochemical properties. In hydrothermal systems, the partitioning of Zn and Cd between sphalerite and parental fluids is controlled by many aspects of parent-fluid geochemistry such as the Zn/Cd ratio, pH, and reduced-sulfur content (Schwartz, 2000; Wen et al., 2016). Variations in fluid Zn/Cd ratios play a key role in determining sphalerite Zn and Cd compositions. Cadmium is strongly correlated with zinc in terms of extraction efficiency from basalt, transport, mixing, sulfide precipitation, and remobilization (Metz and Trefry, 2000). Gottesmann and Kampe (2007) suggested that ores at Tumurtijn-ovoo (Mongolia) with Zn/Cd ratios of >500 were inherited from a basaltic source with similar Zn/Cd ratios, indicating that the Zn/Cd ratio is a useful geochemical indicator for tracking metal sources and/or classifying types of Zn–Pb deposit (Jonasson and Sangster, 1978; Viets et al., 1992; Gottesmann and Kampe, 2007; Demir et al., 2013; Zhu et al., 2016; Wen et al., 2016).

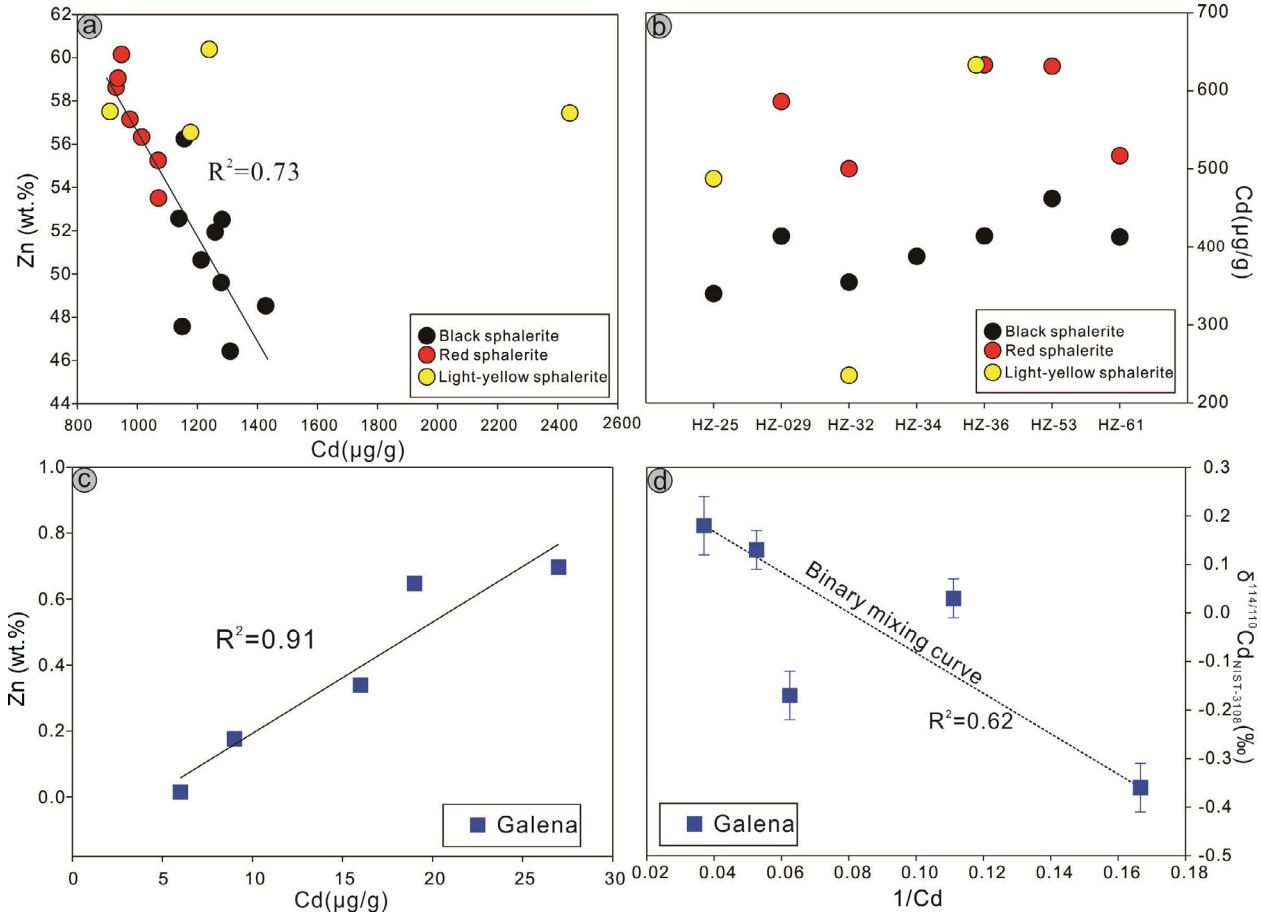

Fig. 5. Plots of (a) Cd–Zn in sphalerite, (b) Cd isotopic compositions of different-colored sphalerite, (c) Cd–Zn in galena, and (d) $\delta^{114/110}$Cd–(1/Cd) for galena.

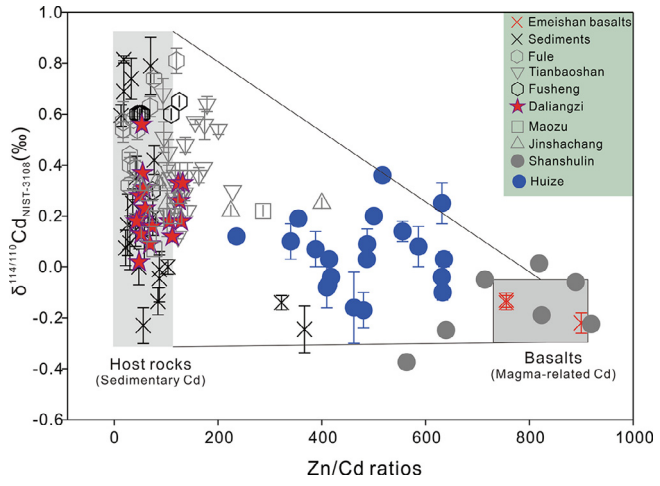

Fig. 6. Plot of Zn/Cd ratios vs. $\delta^{114/110}$Cd values in sphalerite associated with sedimentary rocks and Emeishan basalts in the Huize ore district, from eight Zn–Pb deposits in the SYG area. Shaded grey and dark areas represent ranges of $\delta^{114/110}$Cd values and Zn/Cd ratios. Data sources: Fule (Zhu et al., 2017); Tianbaoshan (Zhu et al., 2016; Xu et al., 2019); Shanshulin (Zhu et al., 2013 and this study); Jinshachang, Maozu, Daliangzi and Fusheng (Xu et al., 2019). Note: Zhu et al. (2013) reported Cd content and isotopic compositions for only sphalerite from the Shanshulin deposit without Zn contents, with more samples being analyzed in this study, as shown in Supplementary Data (Table S4).

In the Huize deposit, the Zn/Cd ratios of sedimentary rocks range from 13 to 367, with most being concentrated in a narrow range of 39–127. In contrast, Emeishan basalts have much higher Zn/Cd ratios (756–900) than sedimentary rocks. Here, the Zn/Cd ratios of sphalerite ranged from 235 to 635 (mean, 479 ± 222; 2SD), much higher than those of sedimentary rocks but lower than those of Emeishan basalts, indicating that Zn and Cd were derived from mixing of fluids extracted from both sedimentary rocks and Emeishan basalts. The REE and C–O isotopic data for the Huize deposit also suggest that the ore-forming fluids were derived from crust–mantle mixing processes, with mantle-derived fluid being related to the Emeishan basalts (Huang et al., 2003, 2004, 2010; Zhang et al., 2005). Recent studies of Zn isotopes indicate that sphalerites of the Huize deposit have $\delta^{66}Zn_{JMC}$ values of 0.17‰–0.32‰ (Wu, 2013), which fall between those of Emeishan basalts (0.30‰–0.44‰) and sedimentary rocks (−0.24‰ to 0.17‰; Zhou et al., 2014), suggesting that Zn was derived from a mixture of sedimentary rocks and the Emeishan basalts.

Based on the geochemical similarities of Zn and Cd, it is reasonable to assume that there is negligible fractionation between Zn and Cd during their extraction from source rocks and the formation of sulfides (Metz and Trefry, 2000). Based on this assumption and the Cd isotopic compositions, we derived a mixing model to explain variations in the Zn/Cd ratios and Cd isotopic compositions of sphalerite in eight large-scale Zn–Pb deposits in the SYG area (Fig. 6) including the Huize, Fule, Tianbaoshan, Daliangzi, Maozu, Jinshachang, and Fusheng deposits. Variations in $\delta^{114/110}$Cd values display a weak (R^2 = 0.44) negative correlation with 1/Cd in sphalerite (Fig. 7a), which is enhanced (R^2 = 0.69) with mean $\delta^{114/110}$Cd and 1/Cd values in different deposits (Fig. 7b). This suggests an isotopic mixing model for the origin of Cd in Zn–Pb deposits in the SYG area, with the Emeishan basalts and sedimentary rocks as the two endmembers. This is consistent with the REE and C, O, and Zn isotopic data as discussed previously (see section 5.1).

The formation ages of the Daliangzi and Fule deposits are 345.2 ± 3.6 Ma (sphalerite and galena; Liu et al., 2018) and 20 ± 3.2 Ma (sphalerite and galena; Liu et al., 2015), respectively, and are distinct from the age of the Emeishan basalts (259–251 Ma; Zhou et al., 2002; Song et al., 2002; Zhong et al., 2014), which suggests that the two deposits had no relationship with the Emeishan basalts during their formation. Indeed, the $\delta^{114/110}$Cd values of these deposits lie in the Zn/Cd range of sedimentary rocks with low Zn/Cd ratios and variable $\delta^{114/110}$Cd values, but beyond the range of Emeishan basalts with higher Zn/Cd ratios and lower $\delta^{114/110}$Cd values (Fig. 6). The age of the Huize deposit is generally considered as 228–223 Ma, based on ^{147}Sm–^{143}Nd (calcite, 228–226 Ma; Li et al., 2007) and ^{87}Rb–^{86}Sr (sphalerite, 226–223 Ma; Yin et al., 2009) dating. These ages are similar to those of native copper mineralization (228–226 Ma; Zhu et al., 2007), which is related to the Emeishan basalts in the Huize area. Li et al. (2007) and Yin et al. (2009) proposed that the Huize deposit was derived from fluid migration during uplift resulting from the Emeishan flood basalts. For other deposits in the SYG area, formation ages are slightly younger than those of the basalts, including the Maozu (calcite, Sm–Nd 196 ± 13 Ma; Zhou et al., 2013b) and Jinshachang (fluorite, Sm–Nd 201 ± 6.2 Ma; Zhang et al., 2015; sphalerite, Rb–Sr, 206.8 ± 3.7 Ma; Zhou et al., 2015) deposits, which have similar mineralization ages, indicating a large mineralization event in this area at ca. 200 Ma. Xu et al. (2014) proposed a thermal simulation model to evaluate the evolution of underplated Emeishan basalts that indicates the release of ore-forming fluid from the basalts occurred over 100 Myr, with a close relationship between Zn–Pb deposits and the Emeishan basalts. We therefore suggest that the metal sources of the Huize and

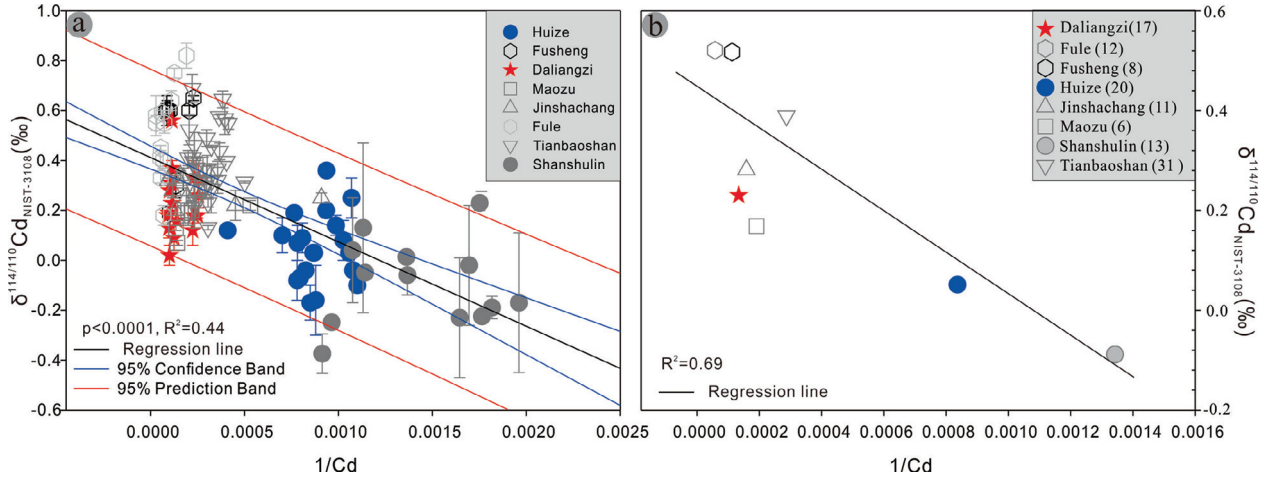

Fig. 7. Plot of average 1/Cd vs. average $\delta^{114/110}$Cd values of sphalerite from eight Zn–Pb deposits in the SYG area. For data sources see Fig. 6 and Supplementary Data (Table S4).

Shanshulin deposits involved a mixture of Emeishan basalts and sedimentary rocks. The basalts might have played a less important role in contributing metals to the Tianbaoshan, Maozu, and Jinshachang deposits, but played a limited role in the formation of the Daliangzi, Fule, and Fusheng deposits.

6. Conclusion

Cadmium isotopic compositions of different-colored sphalerite and sedimentary rocks were investigated to track the Cd isotopic geochemistry and its sources in a large hydrothermal system. Kinetic isotopic fractionation resulted in dark sphalerite (Stage I) having lower $\delta^{114/110}$Cd values than red sphalerite (Stage II). Large variations in fluid temperature might have caused the light-yellow sphalerite (Stage III) to have lower $\delta^{114/110}$Cd values than the dark and red sphalerites. Light Cd isotopes are preferentially enriched in galena over sphalerite. Zn/Cd ratios and Cd isotope compositions of sulfides lie in the range of Emeishan basalts and sedimentary rocks, which are the two potential sources of ore-forming metals and fluids in the Huize ore deposits. In addition, we also summarize the reported data of ore deposits from the SYG area which show that the mean $\delta^{114/110}$Cd values have a good negatively correlation with 1/Cd in sphalerite from these deposits, suggesting an isotopic mixing model for the origin of Cd in Zn–Pb deposits in the SYG area.

We suggest that Cd isotopes can be used as a new geochemical tracer to elucidate the ore genesis of large Pb–Zn hydrothermal systems such as those in the SYG area.

Declaration of Competing Interest

The authors declare that they have no known competing financial interests or personal relationships that could have appeared to influence the work reported in this paper.

Acknowledgments

This project was financially supported by the National Natural Science Foundation of China (Nos. 41773012, 42073010), a special fund managed by the State Key Laboratory of Ore Deposit Geochemistry, Chinese Academy of Sciences, and Science and Technology Foundation of Guizhou Province ([2019]1459).

Appendix A. Supplementary data

Supplementary data to this article can be found online at https://doi.org/10.1016/j.gsf.2021.101241.

References

Abouchami, W., Galer, S.J.G., de Baar, H.J.W., Alderkamp, A.C., Middag, R., Laan, P., Feldmann, H., Andreae, M.O., 2011. Modulation of the Southern Ocean cadmium isotope signature by ocean circulation and primary productivity. Earth Planet. Sci. Lett. 305, 83–91.

Abouchami, W., Galer, S.J.G., Horner, T.J., Rehkämper, M., Wombacher, F., Xue, Z.C., Lambelet, M., Gault-Ringold, M., Stiring, C.H., Schönbächler, M., Shiel, A.E., Weis, D., Holdship, P.F., 2013. A common reference material for cadmium isotope studies—NIST SRM 3108. Geostand. Geoanal. Res. 3, 5–17.

Abouchami, W., Galer, S.J.G., de Baar, H.J.W., Middag, R., Vance, D., Zhao, Y., Klunder, M., Mezger, K., Feldmann, H., Andreae, M.O., 2014. Biogeochemical cycling of cadmium isotopes in the Southern Ocean along the Zero Meridian. Geochim. Cosmochim. Acta 127, 348–367.

Chrastný, V., Čadková, E., Vaněk, A., Teper, L., Cabala, J., Komárek, M., 2015. Cadmium isotope fractionation within the soil profile complicates source identification in relation to Pb–Zn mining and smelting processes. Chem. Geol. 405, 1–9.

Cloquet, C., Carignan, J., Libourel, G., Sterckeman, T., Perdrix, E., 2006. Tracing source pollution in soils using cadmium and lead isotopes. Environ. Sci. Technol. 40, 2525–2530.

Cook, N.J., Ciobanu, C.L., Pring, A., Pring, A., Skinner, W., Shimizu, M., Danyushevsky, L., Saini-Eidukat, B., Melcher, F., 2009. Trace and minor elements in sphalerite: A LA-ICPMS study. Geochim. Cosmochim. Acta 73, 4761–4791.

Demir, Y., Uysal, İ., Sadıklar, M.B., 2013. Mineral chemical investigation on sulfide mineralization of the Istala deposit, Gümüşhane, NE-Turkey. Ore Geol. Rev. 53, 306–317.

Gao, B.o., Liu, Y., Sun, K.e., Liang, X., Peng, P., Sheng, G., Fu, J., 2008. Precise determination of cadmium and lead isotopic compositions in river sediments. Anal. Chim. Acta 612, 114–120.

George, L., Cook, N.J., Ciobanu, C.L., Wade, B.P., 2015. Trace and minor elements in galena: A reconnaissance LA-ICP-MS study. Am. Miner. 100, 548–569.

Georgiev, S.V., Horner, T.J., Stein, H.J., Hannah, J.L., Bingen, B., Rehkämper, M., 2015. Cadmium-isotopic evidence for increasing primary productivity during the Late Permian anoxic event. Earth Planet. Sci. Lett. 410, 84–96.

Gottesmann, W., Kampe, A., 2007. Zn/Cd ratios in calcsilicate-hosted sphalerite ores at Tumurtijn-ovoo, Mongolia. Chem Erde-Geochem. 67, 323–328.

Graeser, S., 1969. Minor elements in sphalerite and galena from Binnatal. Contrib. Mineral. Petrol. 24, 156–163.

Han, R.S., Liu, C.Q., Huang, Z.L., Chen, J., Ma, D.Y., Lei, L., Ma, G.-S., 2007. Geological features and origin of the Huize carbonate-hosted Zn–Pb–(Ag) district, Yunnan, South China. Ore Geol. Rev. 31, 360–383.

Han, R.-S., Chen, J., Wang, F., Wang, X.-K., Li, Y., 2015. Analysis of metal–element association halos within fault zones for the exploration of concealed orebodies—A case study of the Qilinchang Zn–Pb–(Ag–Ge) deposit in the Huize mine district, northeastern Yunnan, China. J. Geochem. Explor. 159, 62–78.

Han, R.S., Li, B., Ni, P., Qiu, W.L., Wang, X.D., Wang, T.G., 2016. Infrared microthermometry of fluid inclusions in sphalerite and geological significance of Huize super-large Zn-Pb-(Ge-Ag) deposit, Yunnan province. Journal of Jilin University (Earth Science Edition) 46, 91–104 (in Chinese with English abstract).

Han, R.S., Wang, F., Zhang, Y., Zhou, G.M., He, J.J., 2017. Metallogenic regularities and deposit type of Rich (Ge-Ag)-Zn-Pb deposits in the Sichuan—Yunnan—Guizhou Triangle (SYGT) area, China. Acta Geol. Sin.-Engl. 91, 208–209.

Hohl, S.V., Galer, S.J.G., Gamper, A., Becker, B., 2017. Cadmium isotope variations in Neoproterozoic carbonates–A tracer of biologic production?. Geochem. Perspect. Let. 3, 32–44.

Hohl, S.V., Jiang, S.Y., Wei, H.Z., Pi, D.H., Liu, Q., Viehmann, S., Galer, S.J., 2019. Cd isotopes trace periodic (bio) geochemical metal cycling at the verge of the Cambrian animal evolution. Geochim. Cosmochim. Acta 263, 195–214.

Horner, T.J., Rickaby, R.E.M., Henderson, G.M., 2011. Isotopic fractionation of cadmium into calcite. Earth Planet. Sci. Lett. 312, 243–253.

Huang, Z.L., Li, W.B., Chen, J., Han, R.S., Liu, C.Q., Xu, C., Guan, T., 2003. Carbon and oxygen isotope constraints on mantle fluid involvement in the mineralization of the Huize super-large Pb-Zn deposits, Yunnan Province, China. J. Geochem. Explor. 78, 637–642.

Huang, Z.L., Chen, J., Han, R.S., Li, W.B., Liu, C.Q., Zhang, Z.L., Ma, D.Y., Gao, D.R., Yang, H.L., 2004. Geochemistry and Ore-formation of the Huize Giant Lead-Zinc Deposit, Yunnan Province, China: Discussion on the Relationship between Emeishan Flood Basalts and Lead-Zinc Mineralization. Geological Publishing House, Beijing, pp. 1–20 (in Chinese).

Huang, Z., Li, X., Zhou, M., Li, W., Jin, Z., 2010. REE and C-O isotopic geochemistry of calcites from the world-class Huize Pb-Zn deposits, Yunnan, China: implications for the ore genesis. Acta Geol. Sin.-Engl. 84, 597–613.

Jonasson, I.R., Sangster, D.F., 1978. Zn/Cd ratios for sphalerites separated from some Canadian sulphide ore samples. Geological Survey of Canada 78, 195–201.

Lacan, F., Francois, R., Ji, Y., Sherrell, R.M., 2006. Cadmium isotopic composition in the ocean. Geochim. Cosmochim. Acta 70, 5104–5118.

Lambelet, M., Rehkämper, M., van de Flierdt, T., Xue, Z., Kreissig, K., Coles, B., Porcelli, D., Andersson, P., 2013. Isotopic analysis of Cd in the mixing zone of Siberian rivers with the Arctic Ocean—New constraints on marine Cd cycling and the isotope composition of riverine Cd. Earth Planet. Sci. Lett. 361, 64–73.

Li, M.L., Liu, S.A., Xue, C.J., Li, D., 2019. Zinc, cadmium and sulfur isotope fractionation in a supergiant MVT deposit with bacteria. Geochim. Cosmochim. Acta 265, 1–18.

Li, Y.G., Zhu, C.W., 2020. The distribution signatures of major and trace elements in zoned sphalerite from lead-zinc deposits: A case study from the Huize deposit. Acta Metall. Sin. https://doi.org/10.16461/j.cnki.1000-4734.2020.40.148 (in Chinese with English abstract).

Liu, M.S., Zhang, Q., Zhang, Y., Zhang, Z., Huang, F., Yu, H.M., 2019. High-precision cd isotope measurements of soil and rock reference materials by MC-ICP-MS with double spike correction. Geostand. Geoanal. Res. 44, 169–182.

Li, W., Huang, Z., Yin, M., 2007. Dating of the giant Huize Zn-Pb ore field of Yunnan Province, Southwest China: constraints from the Sm-Nd system in hydrothermal calcite. Resour. Geol. 57, 90–97.

Liu, Y., Qi, L., Gao, J., Ye, L., Huang, Z., Zhou, J., 2015. Re-Os dating of galena and sphalerite from lead-zinc sulfide deposits in Yunnan Province, SW China. J. Earth Sci.-China 26, 343–351.

Liu, W., Zhang, X., Zhang, J., Jiang, M., 2018. Sphalerite Rb-Sr dating and in situ sulfur isotope analysis of the Daliangzi lead-zinc deposit in Sichuan Province, SW China. J. Earth Sci.-China 29, 573–586.

Metz, S., Trefry, J.H., 2000. Chemical and mineralogical influences on concentrations of trace metals in hydrothermal fluids. Geochim. Cosmochim. Acta 64, 2267–2279.

O'Neil, J.R., 1977. Stable isotopes in mineralogy. Phys. Chem. Miner. 2, 105–123.

Palero-Fernández, F.J., Martín-Izard, A., 2005. Trace element contents in galena and sphalerite from ore deposits of the Alcudia Valley mineral field (Eastern Sierra Morena, Spain). J. Geochem. Explor. 86, 1–25.

Rehkämper, M., Wombacher, F., Horner, T.J., Xue, Z.C., 2012. Natural and anthropogenic Cd isotope variations. In: Baskaran, M. (Ed.), Handbook of Environmental Isotope Geochemistry. Springer, Berlin Heidelberg, pp. 125–154.
Ripperger, S., Rehkämper, M., Porcelli, D., Halliday, A.N., 2007. Cadmium isotope fractionation in seawater—A signature of biological activity. Earth Planet. Sci. Lett. 261, 670–684.
Ripperger, S., Rehkämper, M., 2007. Precise determination of cadmium isotope fractionation in seawater by double spike MC-ICPMS. Geochim. Cosmochim. Acta 71, 631–642.
Schmitt, A.D., Galer, S.J., Abouchami, W., 2009a. High-precision cadmium stable isotope measurements by double spike thermal ionization mass spectrometry. J. Anal At. Spectrom 24, 1079–1088.
Schmitt, A.-D., Galer, S.J.G., Abouchami, W., 2009b. Mass-dependent cadmium isotopic variations in nature with emphasis on the marine environment. Earth Planet. Sci. Lett. 277, 262–272.
Schwartz, M.O., 2000. Cadmium in zinc deposits: Econ. Geol. of a polluting element. Int. Geol. Rev. 42, 445–469.
Song, X.Y., Hou, Z., Wang, Y.L., Zhang, C.J., Cao, Z.M., Li, Y.G., 2002. The mantle plume features of Emeishan basalts. J. Mineral. Petrol. Sci. 22, 27–32 (in Chinese with English abstract).
Tan, D., Zhu, J.-M., Wang, X., Han, G., Lu, Z., Xu, W., 2020. High-sensitivity determination of Cd isotopes in low-Cd geological samples by double spike MC-ICP-MS. J. Anal. At. Spectrom. 35, 713–727.
Tauson, V.L., Parkhomenko, I.Y.u., Babkin, D.N., Men'shikov, V.I., Lustenberg, E.E., 2005. Cadmium and mercury uptake by galena crystals under hydrothermal growth: A spectroscopic and element thermo-release atomic absorption study. Eur. J. Mineral. 17, 599–610.
Viets, J.G., Hopkins, R.T., Miller, B.M., 1992. Variations in minor and trace metals in sphalerite from Mississippi valley-type deposits of the Ozark region; genetic implications. Econ. Geol. 87, 1897–1905.
Wasylenki, L.E., Swihart, J.W., Romaniello, S.J., 2014. Cadmium isotope fractionation during adsorption to Mn oxyhydroxide at low and high ionic strength. Geochim. Cosmochim. Acta 140, 212–226.
Wei, R.F., Guo, Q.J., Wen, H.J., Liu, C.Q., Yang, J.X., Peters, M., Hu, J., Zhu, G.X., Zhang, H.Z., Tian, L.Y., Han, X.K., Ma, J., Zhu, C.W., Wan, Y.X., 2016. Fractionation of Stable Cadmium Isotopes in the Cadmium Tolerant Ricinus communis and Hyperaccumulator Solanum nigrum. Sci. Rep. 6, 1–9.
Wen, H., Zhang, Y., Cloquet, C., Zhu, C., Fan, H., Luo, C., 2015. Tracing sources of pollution in soils from the Jinding Pb–Zn mining district in China using cadmium and lead isotopes. Appl. Geochem. 52, 147–154.
Wen, H.J., Zhu, C.W., Zhang, Y.X., Cloquet, C., Fan, H.F., Fu, S.H., 2016. Zn/Cd ratios and cadmium isotope evidence for the classification of lead-zinc deposits. Sci. Rep. 6, 25273.
Wiggenhauser, M., Bigalke, M., Imseng, M., Müller, M., Keller, A., Murphy, K., Kreissig, K., Rehkämper, M., Wilcke, W., Frossard, E., 2016. Cadmium isotope fractionation in soil-wheat systems. Environ. Sci. Technol. 50, 9223–9231.
Wombacher, F., Rehkämper, M., Mezger, K., Münker, C., 2003. Stable isotope compositions of cadmium in geological materials and meteorites determined by multiple-collector ICPMS. Geochim. Cosmochim. Acta 67 (23), 4639–4654.
Wombacher, F., Rehkämper, M., Mezger, K., 2004. Determination of the mass-dependence of cadmium isotope fractionation during evaporation. Geochim. Cosmochim. Acta 68, 2349–2357.
Wombacher, F., Rehkämper, M., Mezger, K., Bischoff, A., Münker, C., 2008. Cadmium stable isotope cosmochemistry. Geochim. Cosmochim. Acta 72, 646–667.
Wu, Y., 2013. The Age and Ore-forming Process of MVT Deposits in the Boundary Area of Sichuan-Yunnan-Guizhou Provinces, Southwest China. Ph.D. thesis, China University of Geosciences (Beijing), p117 (in Chinese with English abstract).
Xu, Y., Huang, Z., Zhu, D., Luo, T., 2014. Origin of hydrothermal deposits related to the Emeishan magmatism. Ore Geol. Rev. 63, 1–8.
Xu, C., Zhong, H., Hu, R.Z., Wen, H.J., Zhu, W.G., Bai, Z.J., Fan, H.F., Li, F.F., Zhou, T., 2019. Sources and ore-forming fluid pathways of carbonate-hosted Pb–Zn deposits in Southwest China: implications of Pb–Zn–S–Cd isotopic compositions. Miner. Depos. 55, 491–513.
Yang, J., Li, Y., Liu, S., Tian, H., Chen, C., Liu, J., Shi, Y., 2014. Theoretical calculations of Cd isotope fractionation in hydrothermal fluids. Chem. Geol. 391, 74–82.
Yang, S.-C., Lee, D.-C., Ho, T.-Y., 2012. The isotopic composition of cadmium in the water column of the South China Sea. Geochim. Cosmochim. Acta 98, 66–77.
Ye, L., Cook, N.J., Ciobanu, C.L., Yuping, L., Qian, Z., Tiegeng, L., Wei, G., Yulong, Y., Danyushevskiy, L., 2011. Trace and minor elements in sphalerite from base metal deposits in South China: a LA-ICPMS study. Ore Geol. Rev. 39, 188–217.
Yin, M., Li, W., Sun, X., 2009. Rb-Sr isotopic dating of sphalerite from the giant Huize Zn-Pb ore field, Yunnan Province, Southwestern China. Chinese J. Geochem. 28, 70–75.
Zaw, K., Peters, S.G., Cromie, P., Burrett, C., Hou, Z., 2007. Nature, diversity of deposit types and metallogenic relations of South China. Ore Geol. Rev. 31, 3–47.
Zhang, C.Q., Wu, Y., Hou, L., Mao, J.W., 2015. Geodynamic setting of mineralization of Mississippi Valley-type deposits in world-class Sichuan–Yunnan–Guizhou Zn–Pb triangle, southwest China: Implications from age-dating studies past in the decade and the Sm–Nd age of Jinshachang deposit. J. Asian Earth Sci. 103, 103–114.
Zhang, Y., Wen, H., Zhu, C., Fan, H., Luo, C., Liu, J., Cloquet, C., 2016. Cd isotope fractionation during simulated and natural weathering. Environ. Pollut. 216, 9–17.
Zhang, Y., Wen, H., Zhu, C., Fan, H., Cloquet, C., 2018. Cadmium isotopic evidence for the evolution of marine primary productivity and the biological extinction event during the Permian-Triassic crisis from the Meishan section, South China. Chem. Geol. 481, 110–118.
Zhang, Z., Huang, Z., Guan, T., Yan, Z., Gao, D., 2005. Study on the multi-sources of ore-forming materials and ore-forming fluids in the Huize lead-zinc ore deposit. Chinese J. Geochem. 24, 243–252.
Zhong, Y.T., He, B., Mundil, R., Xu, Y.G., 2014. CA-TIMS zircon U-Pb dating of felsic ignimbrite from the Binchuan section: implications for the termination age of Emeishan large igneous province. Lithos 204, 14–19.
Zhou, C., Wei, C., Guo, J., Li, C., 2001. The source of metals in the Qilinchang Zn-Pb deposit, northeastern Yunnan, China: Pb-Sr isotope constraints. Econ. Geol. 96, 583–598.
Zhou, J., Huang, Z., Zhou, M., Li, X., Jin, Z., 2013a. Constraints of C-O–S–Pb isotope compositions and Rb–Sr isotopic age on the origin of the Tianqiao carbonate-hosted Pb–Zn deposit, SW China. Ore Geol. Rev. 53, 77–92.
Zhou, J., Huang, Z., Yan, Z., 2013b. The origin of the Maozu carbonate-hosted Pb–Zn deposit, southwest China: constrained by C-O–S–Pb isotopic compositions and Sm–Nd isotopic age. J. Asian Earth Sci. 73, 39–47.
Zhou, J.X., Huang, Z.L., Zhou, M.F., Zhu, X.K., Muchez, P., 2014. Zinc, sulfur and lead isotopic variations in carbonate-hosted Pb–Zn sulfide deposits, southwest China. Ore Geol. Rev. 58, 41–54.
Zhou, J.X., Bai, J.H., Huang, Z.L., Zhu, D., Yan, Z.F., Lv, Z.C., 2015. Geology, isotope geochemistry and geochronology of the Jinshachang carbonate-hosted Pb–Zn deposit, southwest China. J. Asian Earth Sci. 98, 272–284.
Zhou, M.-F., Malpas, J., Song, X.-Y., Robinson, P.T., Sun, M., Kennedy, A.K., Lesher, C. M., Keays, R.R., 2002. A temporal link between the Emeishan large igneous province (SW China) and the end-Guadalupian mass extinction. Earth Planet. Sci. Lett. 196, 113–122.
Zhu, B.Q., Hu, Y.G., Zhang, Z.W., Cui, C.J., Dai, T.M., Chen, G.H., Peng, J.H., Sun, Y.G., Liu, D.H., Chang, X.Y., 2007. Geochemistry and geochronology of native copper mineralization related to the Emeishan flood basalts, Yunnan Province, China. Ore Geol. Rev. 32, 366–380.
Zhu, C., Wen, H., Zhang, Y., Fan, H., Fu, S., Xu, J., Qin, T., 2013. Characteristics of Cd isotopic compositions and their genetic significance in the lead-zinc deposits of SW China. Sci. China Ser. D 56, 2056–2065.
Zhu, C.W., Wen, H.J., Zhang, Y.X., Liu, Y.Z., Wei, R.F., 2015. Isotopic geochemistry of cadmium: A review. Acta Geol. Sin.-Engl. 89, 2048–2057.
Zhu, C., Wen, H., Zhang, Y., Fan, H., 2016. Cadmium and sulfur isotopic compositions of the Tianbaoshan Zn–Pb–Cd deposit, Sichuan Province, China. Ore Geol. Rev. 76, 152–162.
Zhu, C., Wen, H., Zhang, Y., Fu, S., Fan, H., Cloquet, C., 2017. Cadmium isotope fractionation in the Fule Mississippi Valley-type deposit, Southwest China. Miner. Depos. 52, 675–686.